Additive Global Noise Delays Turing Bifurcations

Axel Hutt* and Andre Longtin
Department of Physics, University of Ottawa, 150 Louis Pasteur, Ottawa, Ontario, K1N-6N5, Canada
Lutz Schimansky-Geier
Humboldt University at Berlin, Institute of Physics, Newtonstrasse 15, 12489 Berlin, Germany
(Received 29 January 2007; published 6 June 2007)

We apply a stochastic center manifold method to the calculation of noise-induced phase transitions in the stochastic Swift-Hohenberg equation. This analysis is applied to the reduced mode equations that result from Fourier decomposition of the field variable and of the temporal noise. The method shows a pitchfork bifurcation at lower perturbation order, but reveals a novel additive-noise-induced postponement of the Turing bifurcation at higher order. Good agreement is found between the theory and the numerics for both the reduced and the full system. The results are generalizable to a broad class of nonlinear spatial systems.

DOI: 10.1103/PhysRevLett.98.230601 PACS numbers: 05.40.−a, 02.30.Jr, 47.20.Ky

The patterns exhibited by real-world dynamical systems are an ongoing subject of intense study, especially because of their relevance in a multitude of experimental contexts. Additive noise [1], and especially multiplicative or ''state-dependent'' noise [2], can alter the bifurcations of simple dynamical systems framed in terms of stochastic differential equations. The analysis of the influence of noise on nonlinear spatially extended systems is a more serious challenge. This problem has received some attention at the theoretical level [3,4] and at the experimental level, e.g., in hydrodynamic systems [5], laser systems [6], in nematic liquid crystals [7], or in neural systems [8]. Since the key point of interest is the effect of noise on nonequilibrium phase transitions, an approach that tracks the behavior of the most unstable mode in terms of the more stable modes and the noise is warranted, a so-called center manifold approach, or relatedly, a slaving approach. A first useful method is to investigate the effect of noise on the bifurcating mode in a heuristic manner [1,9]. More rigorous methods have been developed for specific models [10]. The stochastic center manifold approach (SCM) [11] directly calculates the center manifold in the presence of noise. Here we show that this approach enables the calculation of changes of stability in Turing patterns near their onset. Our work further reveals that additive global noise, which is white in time, has a stabilizing effect on the homogeneous state; i.e., it postpones the onset of the Turing pattern. Such effects have been reported for multiplicative global noise [7], while for additive spatiotemporal white noise, previous studies revealed no such postponement [2]. Our results underscore the importance of extending the center manifold calculations to sufficiently high order for this substantial effect to be seen.

Our method first expands the stochastic partial differential equation (SPDE) of interest into coupled stochastic mode equations, and subsequently applies the SCM analysis. This yields a reduced set of equations involving colored noise, and this system is reduced to an order parameter equation by an adiabatic elimination. We then confirm the analytical results by numerical simulations of both the reduced mode equations and the original full SPDE.

We examine the stochastic Swift-Hohenberg equation [12]

$$\frac{\partial \Psi(x,t)}{\partial t} = \varepsilon \Psi(x,t) - \Psi^3(x,t) - \left(1 + \frac{\partial^2}{\partial x^2}\right)^2 \Psi(x,t) + \sqrt{D'}\xi(t), \tag{1}$$

with periodic boundary conditions, where Ψ is the real field amplitude, and the random Gaussian fluctuations $\xi(t)$

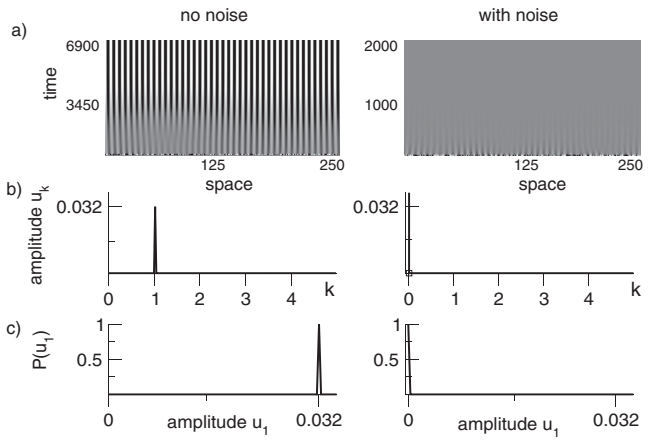

FIG. 1. Effects of global fluctuations on the system Eq. (1). (a) The spatiotemporal activity subtracted by its spatial average is shown without ($D' = 0$, left) and with additive noise ($D' = 6.25 \times 10^{-4}$, right). (b) shows the stationary probability density $P(u_c)$ of the Fourier amplitudes u_c at wave number $k = 1$ computed in the time interval $t \in [13\,500; 13\,600]$ for both noise variances. A stochastic Runge-Kutta algorithm of second order was used for the time integration with a time step $dt = 0.005$ over a spatial grid of 400 elements, $\varepsilon = 0.001$.

obey $\langle \xi(t) \rangle = 0$, $\langle \xi(t)\xi(\tau) \rangle = 2\delta(t-\tau)$; i.e., $\xi(t)$ are uncorrelated in time and constant in space. In the following we refer to $\xi(t)$ as global fluctuations. Figure 1(a) shows the spatiotemporal dynamics of (1) and we observe a spatially periodic pattern with wave number $k = 1$ for the deterministic case $D' = 0$ for large times. In contrast, the additive global fluctuations with $D' \neq 0$ stabilize the homogeneous state; i.e., no prominent pattern is observed. Moreover, the probability density of the spatial Fourier amplitude $u_c = u(k = 1)$ has been computed from the simulated data over a large time interval in the stationary regime [Fig. 1(b)]. We recognize a narrow distribution at the Fourier amplitude value $u_c = 0.032$ and the amplitude value $u_c = 0$ for $D' = 0$ and $D' = 6.25 \times 10^{-4}$, respectively.

The rest of this Letter is devoted to an analytic derivation of this dramatic effect. We introduce the discrete spatial Fourier transform u_n with $\Psi(x,t) = \sum_{n=-\infty}^{\infty} u_n(t) e^{ik_n x}/\sqrt{|\Omega|}$ at discrete values $k_n = n2\pi/|\Omega|$, where Ω denotes the spatial domain. Inserting the Fourier expansion yields the infinite number of stochastic differential equations

$$du_n(t) = \left(\alpha_n u_n(t) - \mu \sum_{l,m} u_l(t) u_m(t) u_{n-l-m}(t) \right) dt + \delta_{n,0} \sqrt{D} dW(t), \tag{2}$$

where $D = D'|\Omega|$, $\alpha_n = \varepsilon - 1 + 2k_n^2 - k_n^4$, $\mu = 1/|\Omega|$, and $dW(t)$ is the differential Wiener process corresponding to the global fluctuations $\xi(t)$. We find $\alpha_n = \alpha_{-n} \in \mathcal{R}$, and since $\Psi(x,t) = \Psi(-x,t)$ it is $u_n = u_{-n} \in \mathcal{R}$. In the following, the stochastic differential equations are interpreted in the Stratonovich sense.

Near the deterministic stability threshold, there is a linear coefficient $\alpha_c = \varepsilon \approx 0$ for the wave number $k_c \approx 1$. This means that the time scale $1/\alpha_c$ of the corresponding amplitude $u_c(t)$ is very large compared to that of the other amplitudes. In the present work, we assume a single amplitude $u_c(t)$ and thus a single value α_c may become positive at a time. Further we will call k_c and the corresponding amplitude u_c the critical wave number and the critical amplitude or order parameter, respectively. By virtue of the time scale separation between amplitudes, the SCM theorem [11,13] allows for the reduction of the number of amplitude Eqs. (2). This theorem states that, near the stability threshold, all stable amplitudes $u_{n \neq c}$ depend on the critical amplitude and the random fluctuations, i.e., $u_{n \neq c}(t) = u_{n \neq c}[u_c(t), t]$. In more physical terms, the amplitude $u_c(t)$ enslaves the other amplitudes [14]. Moreover, assuming the parameters α_c and $\sqrt{D}$ are on the order of the control parameter ε with $\varepsilon \ll 1$, while the other parameters $\alpha_{n \neq c} \sim O(1)$ are large, previous examinations of the deterministic Swift-Hohenberg equation at the lowest order in ε [14] have shown the scaling of the amplitudes $u_c \sim O(\varepsilon^{1/2})$, u_0, u_{2c}, u_{3c}, $\ldots \sim O(\varepsilon)$, and $u_j \sim O(\varepsilon^{3/2})$ for all $j \neq 0$, $2c$, $3c$, $\ldots$. Here $u_{2c}, u_{3c}, \ldots$ denote the amplitudes with wave numbers $k = 2k_c, 3k_c, \ldots$.

The SCM approach allows for the derivation of an evolution equation of the order parameter at specific orders of ε. It is important to note that the treatment of high orders $O(\varepsilon^n)$ leads to a better approximation of the dynamics. Consequently, our analysis starts at low orders of ε, and improves by increasing the order in subsequent steps. Since the time scale of the constant mode $1/|\alpha_0|$ is much larger than that of the amplitudes $u_{2c}, u_{3c}, \ldots$ and the latter relax much faster than $u_0(t)$ and $u_c(t)$. Thus all amplitudes besides $u_0(t)$ and $u_c(t)$ are neglected in the subsequent analytical study.

At the low order $O(\varepsilon^{3/2})$, the application of the SCM approach yields:

$$u_0(t) = \sqrt{D} Z_0(t), \qquad Z_0(t) = \int_{-\infty}^{t} e^{\alpha_0(t-\tau)} dW_0(\tau). \tag{3}$$

We observe that $u_0(t)$ obeys a noise process $Z_0(t)$ with correlation time $1/\alpha_0$, i.e., $Z_0(t)$ is an Ornstein-Uhlenbeck process. Inserting Eq. (3) into Eq. (2), we obtain $du_c = (\alpha_c u_c - 2\mu u_c^3)dt$. This amplitude equation is independent of the colored noise and shows accordance to the well-known deterministic result [12]: if $\alpha_c < 0$, the system is stable and the stationary amplitude of the critical mode vanishes with $u_{\text{stat}} = 0$, i.e., no spatial pattern occurs. In contrast, $\alpha_c > 0$ yields $u_{\text{stat}}^2 = \alpha_c/2\mu > 0$ and the spatial pattern occurs; cf. Fig. 1(a). Thus the additive global fluctuations do not affect the stability of the amplitude $u_c(t)$ at low order $O(\varepsilon^{3/2})$. Now let us examine the next higher nonlinear orders. At $O(\varepsilon^2)$, the SCM approach yields the same amplitude equations as for $O(\varepsilon^{3/2})$. However, important modifications occur at $O(\varepsilon^{5/2})$. It turns out that the stochastic center manifold u_0 remains the same as in the lower orders, while the critical amplitude becomes

$$du_c = [\alpha_c u_c - 3\mu D Z_0^2(t) u_c - 2\mu u_c^3]dt, \tag{4}$$

$$dZ_0 = \alpha_0 Z_0 dt + dW_0(t). \tag{5}$$

In contrast to the lower orders, now the critical amplitude depends on the colored noise process and explicitly on the noise variance D. In other words, we observe a noise-dependent effect of the additive global fluctuations on the critical amplitude.

To arrive at a final order parameter equation, the system (4) and (5) must be reduced to a single order parameter equation. However, the further additional application of the SCM approach does not allow for the further reduction of the equations, as Z_0 does not depend on u_c and the system obtained consequently represents an irreducible form with respect to the Fourier amplitudes [13]. Subsequently, we choose a complementary approach to obtain this single equation, which does not apply directly to the Fourier amplitudes. In a recent study [15], Drolet and Vinal pro-

posed an adiabatic elimination approach for Fokker-Planck equations, which allows for dimensionality reduction near the stability threshold. After introducing the scale-independent variables $\bar{u}_c = u_c/\varepsilon^{1/2}$, $\bar{D} = D/\varepsilon^2$, $\bar{\alpha}_c = \alpha_c/\varepsilon$ with Z_0, α_0, $\mu \sim O(1)$, the Fokker-Planck equation (FP) associated with Eqs. (4) and (5) can be formulated for the time-dependent joint probability density $P(\bar{u}_c, Z_0, t)$. Then the integration over Z_0 of the Fokker-Planck equation (assuming natural boundary conditions) yields the evolution equation of the probability density $P(\bar{u}_c, t)$:

$$\frac{\partial P(\bar{u}_c, t)}{\partial t} = -\frac{\partial}{\partial \bar{u}_c}(\bar{\alpha}_c \bar{u}_c - 2\mu \bar{u}_c^3)\varepsilon P(\bar{u}_c, t) + 3\mu \bar{D}\frac{\partial}{\partial \bar{u}_c}\bar{u}_c \langle Z_0^2|\bar{u}_c\rangle \varepsilon^2, \quad (6)$$

$$\langle Z_0^2|\bar{u}_c\rangle = \int_{-\infty}^{\infty} Z_0^2 P(\bar{u}_c, Z_0, t) dZ_0. \quad (7)$$

We observe that $P(\bar{u}_c, t)$ evolves on two slow time scales of order $O(\varepsilon)$ and $O(\varepsilon^2)$. Further, the integration of the FP for $P(\bar{u}_c, Z_0, t)$ over $\bar{u}_c$ yields the evolution equation of the probability density $P(Z_0, t)$. It turns out that $P(Z_0, t)$ evolves on the fast time scale $O(1)$. Consequently, the probability densities of the amplitudes u_c and Z_0 evolve on different time scales, and thus reflect the time scale separation of the amplitudes. The adiabatic elimination procedure assumes that the conditional probability density $P(Z_0|\bar{u}_c, t) = P(\bar{u}_c, Z_0, t)/P(\bar{u}_c, t)$ evolves on the time scale $O(1)$ by virtue of this time scale separation and thus assumes $\partial P(\bar{u}_c, t)/\partial t \approx 0$. In other words, the processes on the fast time scale of order $O(1)$ experience an almost stationary probability density $P(\bar{u}_c, t)$. One then finds the FP for $P(Z_0|\bar{u}_c, t)$, which evolves at time scale $O(1)$ with the stationary solution $P_s(Z_0|\bar{u}_c) \sim \mathcal{N}(0, 1/|\alpha_0|)$ and we may write $P(\bar{u}_c, Z_0, t) = P_s(Z_0|\bar{u}_c)P(\bar{u}_c, t)$. Inserting this result into Eq. (7) yields $\langle Z_0^2|\bar{u}_c\rangle = 1/|\alpha_0| P(\bar{u}_c, t)$ and the final Fokker-Planck equation of the order parameter (6) reads

$$\frac{\partial P(u_c, t)}{\partial t} = -\frac{\partial}{\partial u_c}[(\alpha_c - \alpha_{th})u_c - 2\mu u_c^3]P(u_c, t), \quad (8)$$

with $\alpha_{\text{th}} = 3\mu D/|\alpha_0| > 0$. At first, we observe that the amplitude $u_c(t)$ is deterministic and approaches the stationary state u_{stat} for large times. In the case $\alpha_c - \alpha_{\text{th}} < 0$, the system is stable and $u_{\text{stat}} = 0$, while $\alpha_c - \alpha_{\text{th}} > 0$ yields the stationary states $u_{\text{stat}} = \pm(\alpha_c - \alpha_{\text{th}})/2\mu$. Moreover, the stability threshold is shifted by α_{th} to larger values. Since this shift depends on the noise variance D, we conclude that the additive global fluctuations yield noise-induced phase transitions and stabilize the homogeneous state of the system. This analytical finding confirms qualitatively the numerical finding in Fig. 1.

In the following we aim to confirm the latter analytical results by numerical simulations. In a first step, the stochastic evolution equations of the amplitudes $u_0(t)$ and $u_c(t)$ taken from Eq. (2) are integrated over several realizations to compute the stationary probability density $P_s(u_c)$. Figure 2 presents $P_s(u_c)$ below and beyond the deterministic threshold for various values of D. We observe $P_s(u_c) = \delta(u_c)$ below the deterministic threshold for all noise variances [Fig. 2(a)]; i.e., the system is stable. In contrast, beyond the deterministic threshold, the stationary probability density $P_s(u_c)$ changes in proportion to D [see Fig. 2(b)]. Specifically, the stationary amplitude shows values $u_c = u_{\text{stat}} \neq 0$ for $D_1 = 0$ and the stationary probability density reads $P_s(u_c) = [\delta(u_c - u_{\text{stat}}) + \delta(u_c + u_{\text{stat}})]/2$. This means the system exhibits a spatial pattern with wave number k_c and amplitude u_{stat}. This case represents the well-known Turing phase transition. Now, increasing D, the stationary amplitude u_{stat} decreases and vanishes for $D \geq D_4$. In other words, the global fluctuations stabilize the system for large noise variances, which shows accordance with the previous analytical results and the numerical findings in Fig. 1. Moreover, the numerical results in Fig. 2 show very good agreement with the analytical results, which highlights the power of the analytical technique.

Further, Fig. 3 shows the stability diagram of u_{stat} with respect to the control parameter $\alpha_c = \varepsilon$ for two noise variances. The absence of random fluctuations, i.e., $D = 0$, yielded the well-known pitchfork bifurcation (left panel in Fig. 3). In contrast, additive global fluctuations shift the bifurcation point to larger values, i.e., it delays the bifurcation, and thus stabilize the system as shown in Fig. 3 for $D = 0.16$. This stability can be observed in Fig. 2 by the probability density $P_s(u_c) = \delta(u_c)$ at this parameter.

Finally we consider the effect of additive global fluctuations in the context of experiments. The experimental study

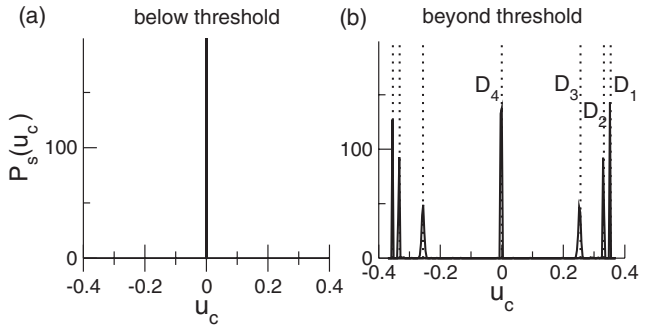

FIG. 2. The stationary probability density $P_s(u_c)$ computed numerically for various values of ε and D and their comparison to analytical results. (a) $\varepsilon = -0.001$, and the system is stable for all D. (b) $\varepsilon = 0.001$ and the system exhibits a single mode with $\alpha_c > 0$. The different probability density functions are computed for $D_1 = 0$, $D_2 = 0.01$, $D_3 = 0.04$, and $D_4 = 0.16$ and the dotted lines represent the analytical results $u_{\text{stat}} = \pm(\alpha_c - \alpha_{\text{th}})/2\mu$. We applied the stochastic Euler forward algorithm with $dt = 0.01$ for the amplitudes $u_c(t)$ and u_0 and computed $P_s(u_c)$ by an ensemble average over 1000 paths after 6×10^5 time steps.

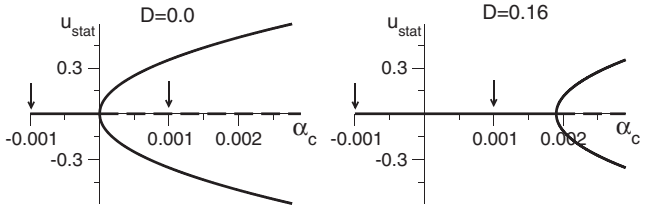

FIG. 3. Bifurcation diagram of the stationary amplitude $u_c = u_{\mathrm{stat}}$ subjected to the control parameter $\alpha_c = \varepsilon$ for two noise variances D. The vertical arrows denote the values of $\alpha_c = \varepsilon$ examined in Fig. 2.

of the Rayleigh-Bénard convection revealed thermal fluctuations at the instability onset, which are uncorrelated in space and time [16]. Since the Swift-Hohenberg equation allows for the modeling of the convective instability near the onset [12], we add the thermal noise $\eta(x, t)$ to Eq. (1):

$$\frac{\partial \Psi(x,t)}{\partial t} = \epsilon\Psi(x,t) - \Psi^3(x,t) - \left(1 + \frac{\partial^2}{\partial x^2}\right)^2 \Psi(x,t) + \sqrt{D'}\xi(t) + \sqrt{D_{th}}\eta(x,t).$$

The global fluctuations $\xi(t)$ are taken from Eq. (1), and the added thermal fluctuations $\eta(x, t)$ with variance D_{th} obey a Gaussian distribution and are uncorrelated in space and time with $\langle \eta(x,t)\rangle = 0, \langle \eta(x,t)\eta(y,\tau)\rangle = 2\delta(x-y)\delta(t-\tau)$. In addition, the global and thermal fluctuations are independent of each other in space and time. Figure 4(a) shows the spatiotemporal activity of the system subject to thermal fluctuations (left panel) and the sum of thermal and global noise (right panel). We observe the stabilization of the system by the global fluctuations even in the presence of thermal fluctuations, as for our previous results without thermal noise. Further, the probability density $P(u_c)$ illustrates the presence and lack of spatially periodic patterns for $D' = 0$ and $D' = 0.25$, respectively [Fig. 4(b)]. These findings lend further support to the results in Figs. 1(a) and 1(b). In summary, thermal noise yields prominent spatial periodic patterns, while the spatially correlated noise leads to spatiotemporal activity which does not show a prominent spatial wave pattern. Hence global fluctuations stabilizes the system even in the presence of thermal fluctuations.

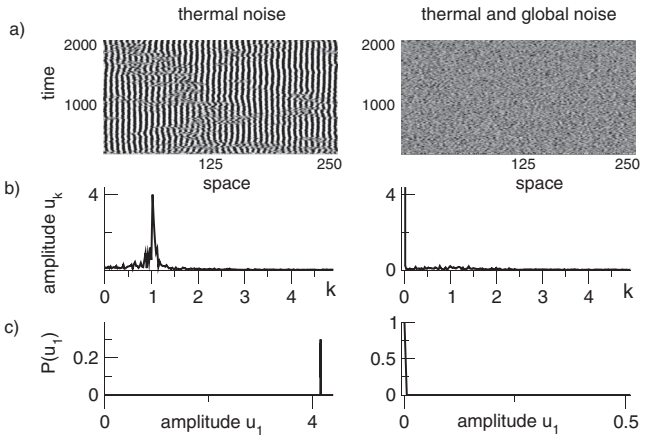

FIG. 4. Effects of global fluctuations in the presence of thermal noise. In (a), the spatiotemporal activity subtracted by its spatial average at each time is shown for thermal noise alone (left panel, $D_{\mathrm{th}} = 2.5 \times 10^{-5}$, $D' = 0$) and for the sum of thermal and strong global fluctuations (right panel, $D_{\mathrm{th}} = 2.5 \times 10^{-5}$, $D' = 0.25$). (b) shows the stationary probability density $P(u_c)$ of the critical Fourier amplitudes u_c computed in the time interval $t \in [35\,000; 35\,100]$ for both noise variances. The same numerical methods and parameters as in Fig. 1 were used.

The present work has focused on the Swift-Hohenberg equation. However the presented combination of two analytical methods can be generalized easily to other pattern forming systems and promises future insights to the effects of additive noise in those systems. Moreover, the work studies fluctuations with no and maximum spatial correlations, while we also expect a delayed bifurcation by spatial noise with an intermediate spatial correlation range.

A. H. and L. S. G. acknowledge the financial support from the Deutsche Forschungsgemeinschaft (Grant No. Sfb-555) and A. L. has been supported by NSERC.

*Electronic address: ahutt@uottawa.ca

[1] E. Knobloch and K. Wiesenfeld, J. Stat. Phys. **33**, 611 (1983).
[2] W. Horsthemke and R. Lefever, *Noise-Induced Transitions* (Springer, Berlin, 1984).
[3] J. Garca-Ojalvo and J. M. Sancho, *Noise in Spatially Extended Systems* (Springer, New York, 1999).
[4] B. Lindner, J. Garcia-Ojalvo, A. Neiman, and L. Schimansky-Geier, Phys. Rep. **392**, 321 (2004).
[5] S. Residori, R. Berthet, B. Roman, and S. Fauve, Phys. Rev. Lett. **88**, 024502 (2001).
[6] O. V. Ushakov, H.-J. Wunsche, F. Henneberger, I. A. Khovanov, L. Schimansky-Geier, and M. A. Zaks, Phys. Rev. Lett. **95**, 123903 (2005).
[7] Th. John, R. Stannarius, and U. Behn, Phys. Rev. Lett. **83**, 749 (1999).
[8] Y. Chen, M. Ding, and J. A. S. Kelso, Phys. Rev. Lett. **79**, 4501 (1997).
[9] T. Frank, A. Daffertshofer, P. Beek, and H. Haken, Physica (Amsterdam) **127D**, 233 (1999).
[10] H. Risken, *The Fokker-Planck Equation-Methods of Solution and Applications* (Springer, Berlin, 1989).
[11] P. Boxler, Probab. Theory Relat. Fields **83**, 509 (1989).
[12] J. B. Swift and P. C. Hohenberg, Phys. Rev. A **15**, 319 (1977).
[13] C. Xu and A. Roberts, Physica (Amsterdam) **225A**, 62 (1996).
[14] H. Haken, *Synergetics* (Springer, Berlin, 2004).
[15] F. Drolet and J. Vinals, Phys. Rev. E **64**, 026120 (2001).
[16] M. Wu, G. Ahlers, and D. S. Cannell, Phys. Rev. Lett. **75**, 1743 (1995).